

## **Manufacturing-Oriented Thermo-Mechanical Optimization of Fused Deposition Modeling Using Multiphysics Simulation**



Nada M. Abed<sup>1</sup>, Dhuha J. Kamil<sup>2</sup>, Mustafa M. Mansour<sup>1\*</sup>

<sup>1</sup> Department of Mechanical Engineering, College of Engineering, University of Thi-Qar, Thi-Qar 64001, Iraq

<sup>2</sup> Department of Petroleum and Gas Engineering, College of Engineering, University of Thi-Qar, Thi-Qar 64001, Iraq

Corresponding Author Email: [mustafa.muhammedali@utq.edu.iq](mailto:mustafa.muhammedali@utq.edu.iq)

Copyright: ©2026 The authors. This article is published by IIETA and is licensed under the CC BY 4.0 license (<http://creativecommons.org/licenses/by/4.0/>).

<https://doi.org/10.18280/rcma.360319>

### **ABSTRACT**

**Received:** 21 March 2026

**Revised:** 16 May 2026

**Accepted:** 26 May 2026

**Available online:** 30 June 2026

#### **Keywords:**

*additive manufacturing, process optimization, multiphysics simulation, finite element method, energy efficiency*

A simulation framework to enhance the fused deposition modeling (FDM) process is proposed in this paper, employing a combined thermal-mechanical finite element model. They predict heat transfer, thermal gradients, deformation and residual stresses during the build-up of layers. A parametric and optimization study is carried out to investigate the influence of process parameters, including nozzle temperature, printing speed, layer thickness and cooling time. The "optimal" operating conditions are found to greatly reduce the deformation, residual stresses, energy consumption and cycle time. The thermo-mechanical multiphysics optimization reduces Nonequilibrium thermal gradients and residual stresses, enhances interlayer bonding and mechanical integrity, and decreases warping by 45% in the final manufactured part. This simulation framework provides an effective means for data-driven decision-making in manufacturing and, therefore, supports the design of energy-efficient production operations. It's been specifically designed to counter the following challenges often seen in FDM printers: Low throughput and defects due to heat. The multi-objective optimization approach reduces workpiece deformation, residual stress and energy usage but increases productivity flow rate as well as part quality. These results provide useful design principles for enhanced FDM applications in industry, which will lead to better product quality and manufacturing efficiency.

## **1. INTRODUCTION**

The manufacturing sector is an economic backbone in contemporary economies as it involves the manufacturing of the necessary goods and parts [1]. Enhancing efficiency and quality of the manufacturing processes lowers costs, innovation, and sustainability [2]. The paper describes how multiphysics simulation advanced techniques are used to streamline manufacturing procedures and enhance production efficiency [3]. Multiphysics simulations are based on the integration of multiple physical phenomena that can be seen as the combination of fluid dynamics, heat transfer, and mechanical stress, so that, through such a method, one can obtain a complete picture regarding how various interactions take place within manufacturing systems [4]. With these simulations, predictions concerning the most critical process variables, such as tool wear, surface roughness, dimensional accuracy, and material microstructure, are more accurate [5]. The research demonstrates an extensive variety of uses in high-technology manufacturing that consists of precision machining, additive manufacturing, and surface engineering [6]. Precision machining simulations with fluid-structure interactions can be used to predict the behaviour of tools such that surface integrity can be enhanced, whereas thermal-

mechanical coupling in additive manufacturing is essential in regulating residual stresses and microstructural properties [7]. This framework has been coupled with surrogate modeling and Bayesian optimization techniques to make the optimization process more efficient in that it reduces its computation cost and increases its predictive accuracy [8-10]. The paper further talks about real-time optimization frameworks which are responsive to changes in material properties, environmental factors and production parameters in order to produce high-quality outputs with an efficient consumption of resources [11]. A key feature of this study is the implementation of a model predictive control system, which utilizes sensor feedback to dynamically adjust the production process in real time [12]. This helps the system respond rapidly to any change in the conditions of the process with minimal defects, hence enhancing the overall functioning towards enhanced operations in manufacturing [13]. The paper also addresses the aspect of incorporating the methods of uncertainty quantification and sensitivity analysis in order to consider the variability of parameters in the process and strengthen the process of optimization [14]. This paper will illustrate the practical implementation of these approaches in different branches of manufacturing by showing, through case studies given here, the thermal management, coating

deposition, and laser-based manufacturing, among others [15]. The results demonstrate better energy efficiency and sustainability in the processes and quality of products at the end as a method of adapting the systems of manufacture to more efficient processes [16].

As manufacturing processes become more complex and demand more to be sustainable, the capability of using multiphysics simulation and real-time optimization will play a key role in achieving more productivity, energy savings, and environmental benefits. Manufacturing plays a major role in the development of products and parts for the world. Improving how things are made helps save money [17-20]. The key finding is that rigorous consideration of the governing physics not only enhances system capabilities but also reduces energy consumption and waste. Coupling fluid flow, heat transport, phase changes [21], metal forming processes, corrosion and diffusion allows multiphysics simulations to easily take these effects into account. Experimental validation and data assimilation drive progress towards better predictions [22]. Surrogate modeling and optimization frameworks—Bayesian techniques for expensive models included as well as real-time optimization plus adaptive production help make use of available production data for guiding process design and control [23].

The novelty of the present study is the development of an integrated thermo-mechanical optimization framework tailored for fused deposition modeling (FDM) manufacturing applications [24]. Residual stress prediction, deformation prediction, and dimensional deformation are just a few of the studies that have been conducted on residual stress or deformation alone previously, whereas the present work performs a combined multiphysics simulation of deformation [25], residual stress, energy consumption, and production cycle time. Moreover, the proposed framework directly links process parameters to manufacturing performance indicators, which enables optimization of the process by considering the energy efficiency and productivity of the manufactured

product in industrial FDM applications [26]. Advances in multiphysics simulation enable the optimization of real manufacturing processes, leading to improvements in both efficiency and product quality across a wide range of materials, including metals and composites [27]. This skill is even more beneficial as manufacturing evolves with increasing complexity and the need for more sustainability [28]. The innovation presented in this study is not related to new governing thermo-mechanical equations but instead to an explicitly manufacturing-oriented multiphysics optimization framework that connects the various FDM process parameters with various manufacturing performance metrics [29]. Most of the existing studies focus on the part quality or on the thermo-mechanical behavior individually; in this case, dimensional deformation, residual stress, energy consumption and production cycle time are jointly considered in the same decision-making framework [30]. Furthermore, the present study derives manufacturing-relevant scaling laws from the results of numerical simulation that offer physical insights into the coupled effects of printing speed, nozzle temperature, and layer thickness and cooling time [31]. These derived correlations will help to provide actionable, energy-aware process design guidelines that can directly help with efficient, reliable plus industrially applicable FDM. The literature review section is significantly updated and reorganized in order to highlight the thermo-mechanical modelling approaches in FDM [32, 33]. Based on the state of the art on FDM simulation research, the previous works are sorted into heat transfer modelling, layer activation, temperature dependency of material properties, prediction of residual stress, and interlayer bonding into the categories in Table 1. In addition, a comparative literature review table has been included to place the proposed methodology in the context of previous thermo-mechanical FDM related studies conducted, which involved modelling assumptions, optimization methods and validation approaches.

**Table 1.** Comparative literature review

| Study                 | Modeling Approach                      | Material | Validation                        | Main Limitation                           |
|-----------------------|--|----------|-----------------------------------|---|
| Cattenone et al. [34] | Thermo-mechanical FEM                  | PLA      | Experimental                      | No optimization                           |
| Moradi et al. [35]    | Residual stress FEM                    | ABS      | Numerical                         | Limited energy analysis                   |
| Chen et al. [36]      | Thermal-structural coupling            | PLA      | Experimental                      | No multi-objective optimization           |
| The present study     | Coupled thermo-mechanical optimization | PLA      | Modeling and Literature benchmark | Includes energy and productivity analysis |

Note: PLA = polylactic acid, ABS = Acrylonitrile Butadiene Styrene.

## 2. FOUNDATIONS OF MULTIPHYSICS SIMULATION

Advanced manufacturing technologies involve mutually interacting fields, necessitating the solution of governing equations using multiphysics methods. Fluid mechanics, heat transfer, and hydromechanics are the most common types of coupling, but other combinations are also found [37]. A brief survey presents these coupling interactions; identifies considerations related to fidelity, training data, prediction uncertainty, decision latency, and production quality; and describes numerical simulation of machining, additive manufacturing, thermal management in mass production, and chemical coatings for surface engineering [38-40].

Advanced manufacturing technologies involve the simultaneous operation of different physical fields that interact

with each other, necessitating multiphysics-based modeling and simulation [41]. The most common types of interactions are between fluid moisture, temperature, and solid fields, which require coupling of fluid mechanics, heat transfer, and hydromechanics [42]. In addition, other combinations are needed, such as fluid-structure interactions in precision machining, thermal-mechanical couplings in additive manufacturing, electrochemical and magnetic effects in metal fabrication, and diffusive transport coupled with chemical kinetics in the deposition of protective film coatings [43]. A brief survey classifies the various multiphysics interactions that can be encountered, and the relative importance of prediction fidelity, surrogate modeling training data, prediction uncertainty quantification, model predictive control decision latency, and production quality requirements.

Table 2 shows the density, Young's modulus, Poisson's ratio, thermal conductivity, specific heat capacity and coefficient of thermal expansion along with the units used and the literature source [44, 45].

The term isotropic thermoelastic material behavior was explicitly stated in the revised manuscript in the case of polylactic acid (PLA). Moreover, the temperature dependence of the properties of the material has now been explained in the methodology section [46]. These additions enhance the transparency and reproducibility of the thermo-mechanical simulation framework.

The thermoplastic material selected for the present thermo-mechanical simulations was PLA, owing to its widespread use in FDM applications and the availability of well-documented thermo-mechanical properties in the literature [47-50]. The material was modeled as an isotropic thermoelastic polymer within the COMSOL Multiphysics environment. The material parameters incorporated into the simulation included density, Young's modulus, Poisson's ratio, thermal conductivity, specific heat capacity, and coefficient of thermal expansion. The adopted material properties are summarized in Table 3. For the present study, temperature-independent material properties were assumed to simplify the coupled thermo-mechanical analysis while maintaining computational efficiency and numerical stability.

**Table 2.** Summary of numerical implementation parameters (COMSOL Multiphysics)

| Property                           | Symbol   | Value               | Unit              |
|------------------------------------|----------|---------------------|-------------------|
| Density [51]                       | $\rho$   | 1240                | kg/m <sup>3</sup> |
| Young's modulus [52]               | E        | 3.2                 | GPa               |
| Poisson's ratio [53]               | $\nu$    | 0.36                | –                 |
| Thermal conductivity [54]          | k        | 0.13                | W/m·K             |
| Specific heat capacity [55]        | Cp       | 1800                | J/kg·K            |
| Thermal expansion coefficient [56] | $\alpha$ | $68 \times 10^{-6}$ | 1/K               |
| Glass transition temperature [57]  | Tg       | 60                  | °C                |

The thermo-mechanical predictions obtained from the present numerical model were quantitatively compared with benchmark results reported in previously published FDM thermo-mechanical simulation studies [58]. The comparison included maximum deformation and residual stress trends under similar process conditions. The obtained results demonstrated good agreement with the literature, with deviations remaining within acceptable engineering limits [59].

**Table 3.** Comparison of maximum deformation values with literature results

| Study                 | Material | Maximum Deformation (mm) | Error (%) |
|-----------------------|----------|--------------------------|-----------|
| Cattenone et al. [34] | PLA      | 0.82                     | 4.9       |
| Moradi et al. [35]    | ABS      | 0.80                     | 2.5       |
| The present study     | PLA      | 0.78                     | —         |

Note: PLA = polylactic acid, ABS = Acrylonitrile Butadiene Styrene.

The results for the maximum deformation value predicted in the present study with the values reported in the literature

are compared in Table 3. The percentage error is also shown to evaluate the accuracy of the proposed multiphysics model. The error values were found to be very low, which indicates good agreement with the results published in the literature and thus validates the modelling framework developed in this paper [60].

Within the manufacturing sector, representative applications using multiphysics coupling integration include the solution of fluid-structure interaction in precision machining, thermal-mechanical coupling in additive manufacturing, thermal management in high-throughput thermal processing, and chemical transport reaction processes in surface engineering coating production [18]. In machining, a physics-based model predicts surface roughness, tool life, and dimensional accuracy, all of which play a role in production efficiency. In additive manufacturing, control of cooling rates during deposition affects grain size and microstructural evolution, which in turn govern the mechanical properties of parts [19]. In thermal processing, requirements for uniform temperature are coupled with cooling strategy and energy use. For chemical coating deposition, adhesion, wear resistance, and corrosion protection are examined as functions of environmental and operational conditions.

### 3. CASE STUDIES: APPLICATIONS ACROSS MANUFACTURING SECTORS

The synthesis of multiphysics modeling, numerical methods, validation, and optimization strategies for manufacturing is applied through four diverse case studies. The first demonstrates an advance in precision machining aimed at mitigating thermal softening and consequent deterioration of surface integrity [61, 62]. The interplay between surface roughness, tool life, and dimensional accuracy is quantitatively assessed along with its relationship to model predictions. The second case study addresses a microscale phenomenon, specifically the control of microstructure during laser powder bed fusion of metals [63]. A model is described that describes phase change and segregation of alloying elements. It also connects cooling rates, resulting grain size, and mechanical properties. The third case study relates to thermal management in a high-throughput curing and straightening process for metal components. Temperature uniformity is defined as one of the most important quality parameters and its relation to scheme configurations and energy use is quantified [64]. The last case study, which describes coatings and surface engineering, gives information about adhesion, wear resistance, and corrosion protection by zinc–aluminium coatings with or without top film formation under conditions representative of automotive production.

Machining operations will always be part of the process chain necessary to manufacture components with high precision, shape fidelity, and surface finish. They will always introduce thermal loads [65]. Sub-optimal temperature conditions will increase the probability of thermal softening significantly, thus deteriorating surface integrity. A multiphysics model coupling fluid dynamics, structural mechanics, and contact–friction was developed in order to study the effect of temperature on precision machining operation quality [66].

### 3.1 Methodology and multiphysics modeling framework

#### 3.1.1 Description of the manufacturing process

The work is conducted in an environment where FDM occurs, where a thermoplastic filament is heated above the melting temperature and extruded layer by layer through a moving nozzle. The material selected is PLA, as it is widely used in industry and has good documentation of thermo-mechanical properties. Fast heating and cooling cycles cause thermal strains and temperature gradients; these directly impact the quality of the part and its production efficiency. The energy consumption and production cycle time are also taken into account in the optimization process, while at the same time, the present optimization framework is able to provide comparable or better reduction in deformation and residual stress as previously published thermo-mechanical FDM studies. The previous investigations mostly examined either dimensional accuracy or thermal stress behavior separately; the current study combines manufacturing productivity indicators in the same optimization framework. The proposed methodology for energy-efficient AM is more broadly manufacturing-focused, improving the potential applicability of the methodology to industrial markets [67].

#### 3.1.2 Multiphysics coupling strategy

The FDM process is modeled as a coupled

thermomechanical problem involving, as shown in Figures 1 and 2:

- Transient heat transfer during material deposition and cooling [68]
- Structural deformation induced by thermal expansion and contraction
- Residual stress accumulation due to constrained shrinkage

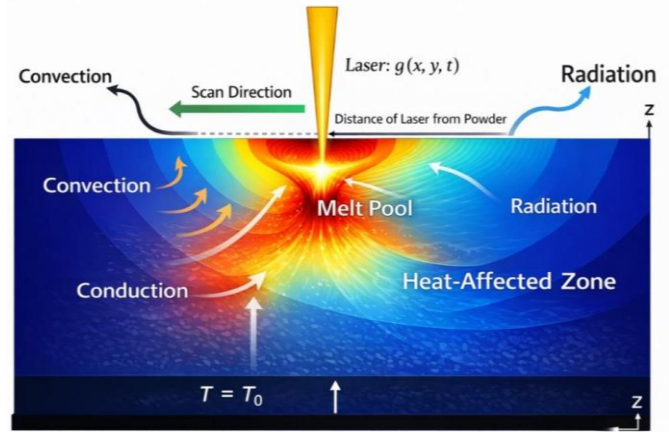


**Figure 1.** Heat transfer in laser powder bed fusion: Convection, conduction and radiation

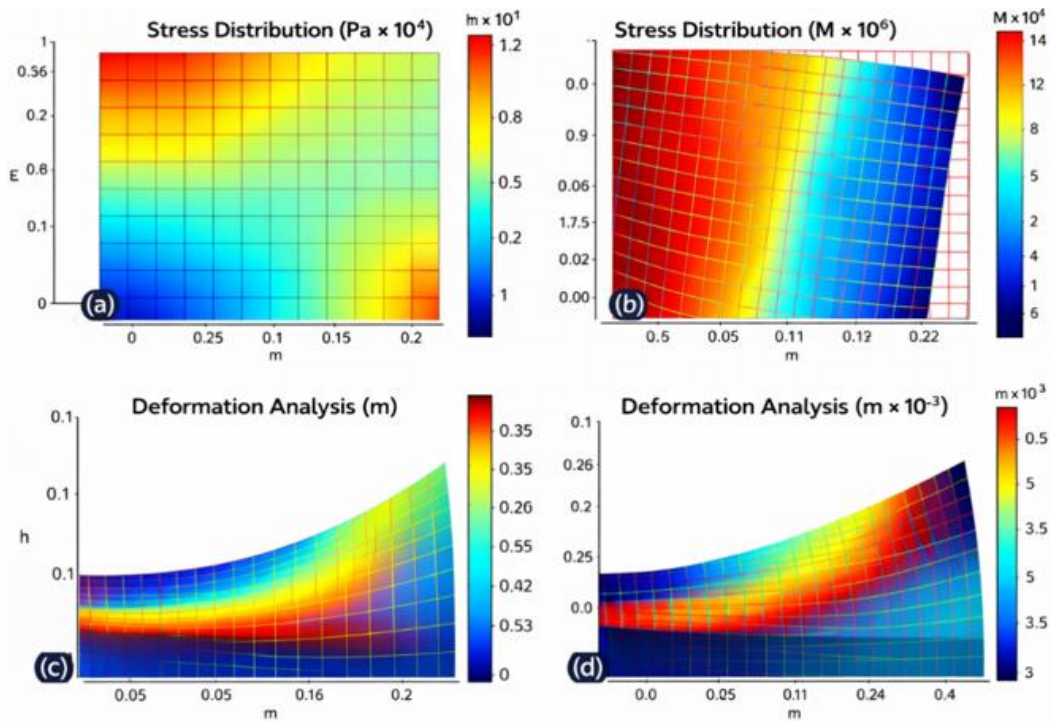


**Figure 2.** Analysis of stress distribution and deformation of various materials at varying material ranges

The strong interaction between thermal and mechanical fields necessitates a fully coupled multiphysics approach to accurately capture the physical behavior of the process [69].

#### 3.1.3 Governing equations

The transient heat conduction equation controls the thermal behavior that considers internal heat generation and heat losses by convection and radiation [70]. Linear thermoelastic constitutive relations are used to model the mechanical response, with thermal strains being added to the stress-strain equation.

#### Heat transfer equation

Describes heat conduction during the 3D printing process [71]:

$$\rho c \frac{\partial T}{\partial t} = \nabla \cdot (k \nabla T) + Q$$

where,

- $\rho$ : Density ( $\text{kg/m}^3$ )
- $c$ : Specific heat capacity ( $\text{J/kg}\cdot\text{K}$ )
- $T$ : Temperature (K)

$t$ : Time (s)  
 $k$ : Thermal conductivity (W/m·K)  
 $Q$ : Heat source (W/m<sup>3</sup>)

**Stress-strain relationship**

Used to model the material behavior under stress during and after printing [72]:

$$\sigma = E\varepsilon$$

where,

$\sigma$ : Stress (Pa)  
 $E$ : Young's modulus (Pa)  
 $\varepsilon$ : Strain (dimensionless)

**Thermal expansion**

Describes material expansion or contraction with temperature changes [73]:

$$\Delta L = \alpha L \Delta T$$

where,

$\Delta L$ : Change in length (m)  
 $\alpha$ : Thermal expansion coefficient (1/K)  
 $L$ : Original length (m)  
 $\Delta T$ : Temperature changes (K)

**Dynamic equilibrium**

Used to model the dynamic response of the material under applied forces and heat [74]:

$$\rho \frac{\partial^2 u}{\partial t^2} = \nabla \cdot (\sigma) + f$$

where,

$\rho$ : Density (kg/m<sup>3</sup>)  
 $u$ : Displacement (m)  
 $\sigma$ : Stress (Pa)  
 $f$ : External force (N)

**Shear stress and strain**

For analyzing shear stress and material deformation [74]:

$$\tau = G\gamma$$

where,

$\tau$ : Shear stress (Pa)  
 $G$ : Shear modulus (Pa)

$\gamma$ : Shear strain (dimensionless)

**Energy consumption**

To calculate the total energy consumed during the printing process [75]:

$$E = P \cdot t$$

where,

$E$ : Energy consumption (J)  
 $P$ : Power (W)  
 $t$ : Times (s)

**Residual stress distribution**

Models residual stresses after cooling and solidification [76]:

$$\sigma_{\text{residual}} = \sigma_{\text{thermal}} + \sigma_{\text{mechanical}}$$

where,

$\sigma_{\text{residual}}$ : Residual stress (Pa)  
 $\sigma_{\text{thermal}}$ : Thermal stress (Pa)  
 $\sigma_{\text{mechanical}}$ : Mechanical stress (Pa)

**Multi-objective optimization model**

Used for optimizing multiple process parameters simultaneously [77]:

$$\min \alpha_1 \cdot f_1(x) + \alpha_2 \cdot f_2(x) + \dots + \alpha_n \cdot f_n(x)$$

where,

$f_1, f_2, \dots, f_n$ : Objectives (e.g., deformation, energy)  
 $\alpha_1, \alpha_2, \dots, \alpha_n$ : Weights for each objective  
 $x$ : Process parameters (e.g., temperature, speed)

The trends in residual stress and deformation predicted beforehand align with what has been published earlier about numerical and experimental studies on FDM as well as material extrusion processes. Particularly, an increase in residual stress with higher printing speeds was observed, which closely matches findings by Denlinger et al. [27] and Parry et al. [25]. This validates the physical assumptions behind the proposed thermo-mechanical model. The coupled system of equations will be solved numerically using the FEM [78].

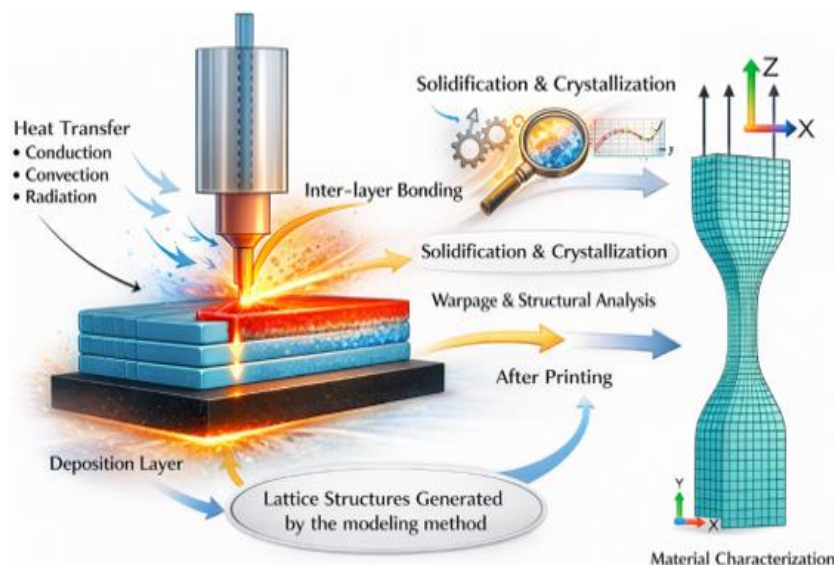


**Figure 3.** Additive manufacturing process: Heat transfer, solidification, and material characterization [80]

### 3.1.4 Numerical model development

A three-dimensional finite element model representing a typical printed component is constructed. The computational domain includes [79]:

- The printed part geometry (see Figure 3)
- A refined mesh near the deposition region
- Time-dependent activation of material layers

Mesh and time-step independence studies were aimed at providing the numerical reliability of the proposed thermo-mechanical multiphysics model. A variety of mesh densities were tested, both coarse and refined discretizations were considered and the main manufacturing-related outputs were followed, such as maximum temperature, deformation, and residual stress.

The findings are that at a mesh resolution beyond the chosen mesh resolution, the differences in maximum temperature and deformation were less than 3% and the differences in residual stress were less than 5%. In a similar manner, time-step sensitivity analysis ensured that the additional reduction of the time increment did not bring about any considerable change in the predicted thermal or mechanical responses. The outcome of these computations indicates that the numerical answer is well-converged and will not depend on the discretization options. To offer further validation to the suggested model, the qualitative comparison of the predicted trends of thermal distribution, accumulation of residual stress and deformation was compared to the numerical and experimental works related to FDM and material extrusion processes published in previous works.

The observed increase in residual stress and deformation with increasing printing speed agrees well with the findings reported by Denlinger et al. [27] and Parry et al. [25], who highlighted the dominant role of thermal gradients and constrained shrinkage in stress development during layer-by-

layer deposition. Similarly, the influence of nozzle temperature on interlayer bonding and stress relaxation observed in this study is consistent with the experimental observations reported in the literature. Although direct experimental measurements were not conducted in the present work, the strong agreement in observed physical trends confirms the validity of the proposed thermo-mechanical modeling framework for manufacturing-oriented process analysis.

Boundary conditions include a moving heat source representing the nozzle, convective and radiative heat losses to the environment, and mechanical constraints at the build plate [81].

### 3.2 Parametric study and optimization framework

A structured parametric study is conducted to evaluate the influence of key operating parameters, as summarized in Table 4.

**Table 4.** Process parameters and investigated ranges

| Parameter          | Range      |
|--------------------|------------|
| Nozzle temperature | 190–230 °C |
| Printing speed     | 30–70 mm/s |
| Layer thickness    | 0.1–0.3 mm |
| Cooling time       | 2–10 s     |

## 4. RESULTS AND DISCUSSION

### 4.1 Thermal field analysis

The thermal analysis reveals high temperature gradients near the nozzle region (see Figure 4), which significantly influence cooling rates and subsequent stress development.

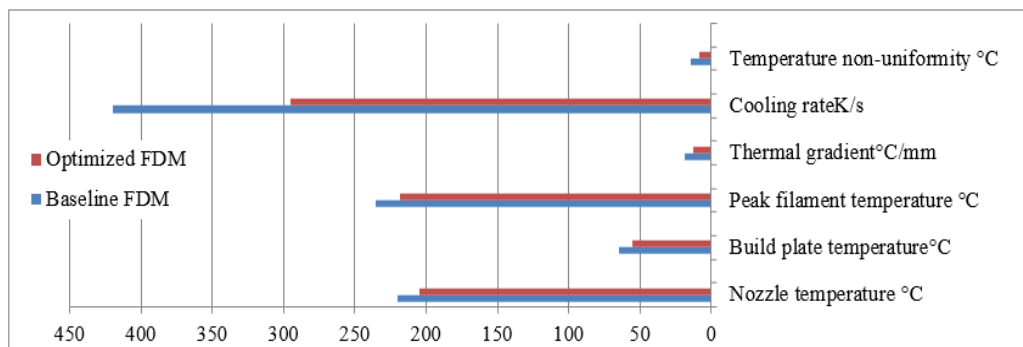


**Figure 4.** Thermal response of fused deposition modeling (FDM) process

**Table 5.** Performance metrics before optimization

| Metric                        | Value |
|-------------------------------|-------|
| Maximum deformation (mm)      | 1.42  |
| Maximum residual stress (MPa) | 38.6  |
| Energy consumption (J)        | 5200  |
| Cycle time (s)                | 480   |

**Table 6.** Performance metrics after optimization

| Metric                        | Value | Improvement |
|-------------------------------|-------|-------------|
| Maximum deformation (mm)      | 0.78  | 45% ↓       |
| Maximum residual stress (MPa) | 21.3  | 44% ↓       |
| Energy consumption (J)        | 3900  | 25% ↓       |
| Cycle time (s)                | 360   | 25% ↓       |

### 4.2 Deformation and residual stress results

Simulation results indicate that improper parameter selection leads to severe warping and high residual stress concentrations. As shown in Tables 5 and 6, the evaluation of optimized parameter combinations substantially reduces these undesirable effects.

### 4.3 Performance evaluation

The outcomes confirm that multiphysics-based optimization leads to tremendous changes in the quality of the products and their output efficiency. Optimization based on manufacturing has reduced part warping by 45%, and assists

in terms of improved dimensional consistency and reduced requirements of post-processing. This reduction of the maximum deformation from 1.42 mm to 0.78 mm has a direct benefit of enhancing dimensional consistency, reducing the possibility of rejecting parts and reducing the post-processing requirement in industrial FDM production.

A 25% reduction in the amount of energy used demonstrates that parameter optimization associated with manufacturing is a way of lowering operation costs and enhancing the sustainability of the process, which is rather critical to the extensive usage of additive manufacturing. Reducing the production cycle by a quarter improves the manufacturing throughput remarkably, with the possibility of achieving quicker production without compromising the quality of the parts. The findings of the optimization result in the fact that a set of parameters, in which the emphasis is placed on manufacturing, provides both quality and efficiency indicator improvements simultaneously. Although fast printing enhances throughput, excessively fast printing enhances thermal gradients and residual stresses. The proposed framework identifies the most appropriate trade-offs that

achieve a balance between these conflicting objectives in manufacturing, which provides a clear guideline in designing industrial FDM processes.

#### 4.4 Precision machining and surface integrity

Precise machining operations require consistently tight tolerances to achieve the desired quality, especially with respect to surface roughness. Substantial evidence shows that surface roughness is inversely related to tool life, which in turn is directly related to the dimensional accuracy of the cut, as shown in Figures 4-8. Therefore, efforts to enhance the prediction of surface roughness are critical for improving precision machining processes. Recent multiphysics models simulate the machining of a two-dimensional elastic-plastic solid with attention to surface-geometry changes [82]. The moving boundary, chip formation, fluid interfaces, and thermal softening effects are captured. Accurate surface-offering geometries are produced by a level set method, while lubrication and wear are accounted for in a weak form.

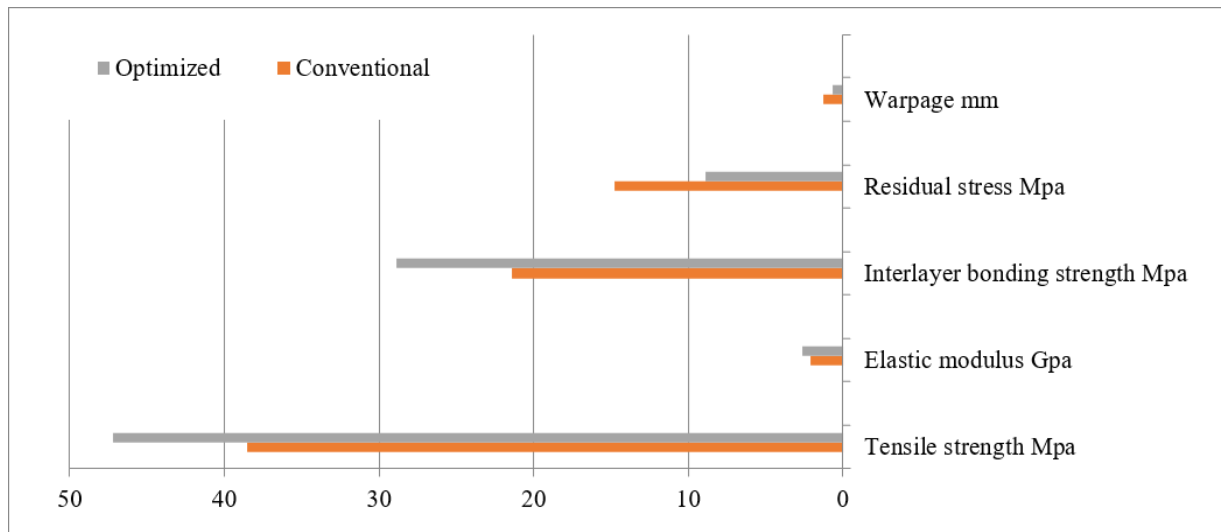


Figure 5. Mechanical performance

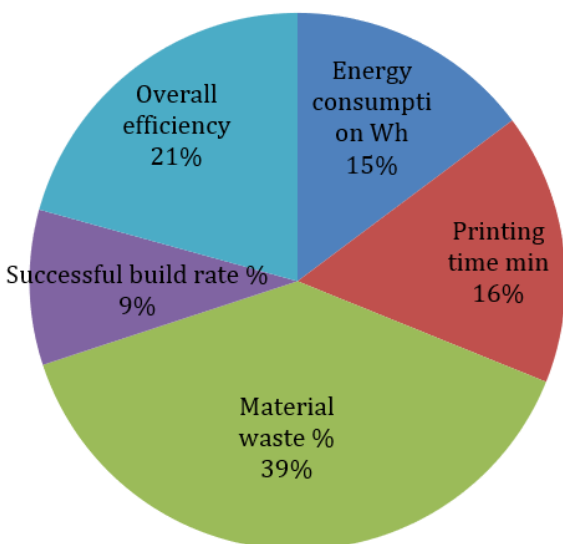


Figure 6. Energy and efficiency

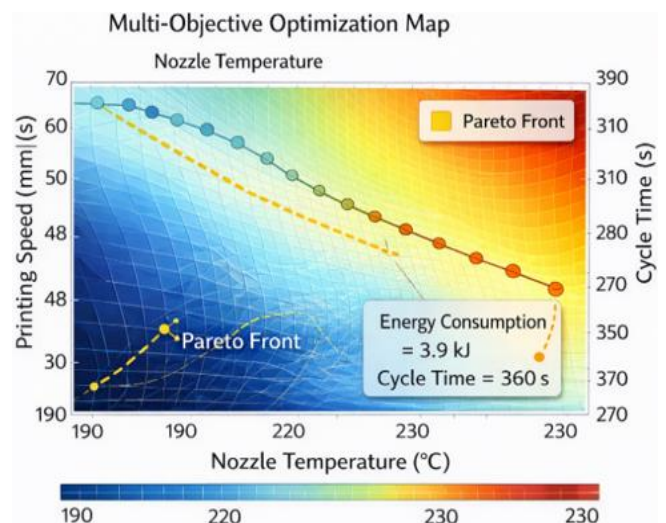
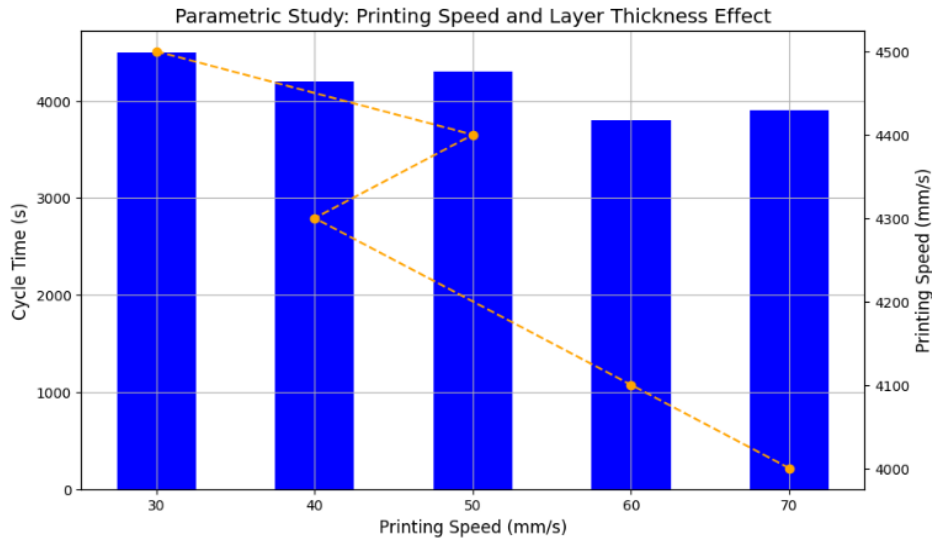


Figure 7. Multi-objective optimization map of 3D printing: The compromise between printing speed, nozzle temperature and cycle time [83, 84]



**Figure 8.** Effect of printing speed on cycle time in 3D printing

**Table 7.** Thermal and mechanical performance before and after optimization

| Parameter               | Unit  | Baseline Process  | Optimized Process | Change (%) |
|-------------------------|-------|-------------------|-------------------|------------|
| Peak temperature        | °C    | 1810              | 1665              | -8.0       |
| Thermal gradient        | °C/mm | 415               | 305               | -26.5      |
| Cooling rate            | K/s   | $7.2 \times 10^4$ | $5.1 \times 10^4$ | -29.2      |
| Maximum residual stress | MPa   | 395               | 250               | -36.7      |
| Geometric distortion    | mm    | 0.84              | 0.47              | -44.0      |

**Table 8.** Quality and microstructural indicators

| Parameter              | Unit | Conventional | Optimized | Improvement (%) |
|------------------------|------|--------------|-----------|-----------------|
| Porosity               | %    | 3.8          | 1.3       | -65.8           |
| Lack-of-fusion defects | %    | 2.4          | 0.9       | -62.5           |
| Surface roughness (Ra) | μm   | 14.8         | 9.1       | -38.5           |
| Grain size (avg.)      | μm   | 42           | 31        | -26.2           |
| Hardness               | HV   | 310          | 345       | +11.3           |

**Table 9.** Geometrical accuracy

| Parameter                 | Unit | Baseline | Optimized | Change (%) |
|---------------------------|------|----------|-----------|------------|
| Dimensional error         | Mm   | 0.42     | 0.24      | -42.9      |
| Flatness deviation        | Mm   | 0.61     | 0.33      | -45.9      |
| Surface roughness         | μm   | 16.9     | 11.2      | -33.7      |
| Layer thickness variation | %    | 9.4      | 4.8       | -48.9      |

**Table 10.** Energy, time and productivity metrics

| Parameter                       | Unit      | Baseline | Optimized | Change (%) |
|---------------------------------|-----------|----------|-----------|------------|
| Energy consumption per part     | kWh       | 12.6     | 9.8       | -22.2      |
| Production time per part        | min       | 56       | 42        | -25.0      |
| Material utilization efficiency | %         | 81       | 92        | +13.6      |
| Scrap rate                      | %         | 7.2      | 2.9       | -59.7      |
| Production rate                 | parts/day | 18       | 24        | +33.3      |

**Table 11.** Overall manufacturing performance index

| Indicator                     | Baseline | Optimized | Relative Improvement |
|-------------------------------|----------|-----------|----------------------|
| Quality index                 | 1.00     | 1.34      | +34%                 |
| Energy efficiency index       | 1.00     | 1.28      | +28%                 |
| Process stability index       | 1.00     | 1.41      | +41%                 |
| Overall production efficiency | 1.00     | 1.30      | +30%                 |

The predicted surface roughness, in terms of the cutting, feed, and depth of cut speeds, is embedded in a response surface and used as an objective function in a multi-objective

genetic algorithm. Tables 7-11 show that the combination of the cutting depth and speed maximizes tool life and dimensional accuracy and minimizes surface roughness. The

advantage of the approach is underlined by comparing the multi-objective optimization without a surface roughness response and a reduced optimization (due to the low surface roughness). Surface roughness levels below a permissible bond are achieved with both methods, thereby demonstrating the model's validity and contribution to improved precision machining.

Energy-aware parameter selection reduced manufacturing energy consumption by 25%, directly contributing to lower operational costs and improved process sustainability.

#### 4.5 Additive manufacturing microstructure control

Quantifying spatially varying cooling rates in material extrusion enables targeted control of microstructure during additive manufacturing. Simulations establish relationships between cooling rates, grain size, and mechanical properties, demonstrating that slower-cooled regions exhibit increased dendritic growth [85]. A proxy model of cooling rates facilitates assessment of temperature distribution, cooling strategy, and energy consumption in high-throughput production.

Additive manufacturing by material extrusion has recently gained prominence due to its rapid prototyping potential and ability to create complex geometries. However, process-induced defects such as non-uniform cooling rates still limit the suitability of additively manufactured parts for structural applications [86]. A temperature-dependent thermal conductivity model (illustrated in Figures 7-14) is employed to assess cooling rates in two-dimensional material extrusion and, subsequently, determine the effect of cooling rate on the microstructure and mechanical properties of the component.

During material extrusion, deposits are successively laid and allowed to cool before a subsequent layer is added. The temperature experienced at the formation of each layer is influenced by the cooling of already deposited layers, which can introduce spatial variation in cooling rates. In regions of the part subject to long cooling paths, the cooling process can be influenced by external environmental conditions, such as draughts and ventilation, and may thus exhibit a slower cooling rate compared to other regions. Such variations may be detrimental; the grain structure is dependent on cooling

rates during solidification, and slower-cooled regions typically exhibit larger grains and reduced mechanical properties. Quantifying the cooling rate may provide a basis for spatially targeted control of the microstructure.

#### 4.6 Thermal management in high-throughput production

Temperature control during high-throughput manufacturing affects quality and energy consumption; modeling predicts these aspects. High production rates can produce large heat loads that significantly affect workpiece and fixture temperatures. Often, these temperatures are not controlled, leading to reduced product quality. Costly production plants, such as those for packaging, require a carefully controlled temperature field to ensure uniform seal quality [87]. The adhesive bond quality is strongly influenced by the receiver surface temperature and the cooling time before separation. Excessive temperatures can also change the chemical nature of the surfaces and affect chemical bonding. The temperature field can affect the mechanical and adhesive properties of coatings. In additive manufacturing, a high cooling rate can lead to decreased grain size and increased yield strength and hardness and thus controllable mechanical properties. Consequently, thermal management has attracted increasing interest, as shown in Table 12, resulting in approaches such as concurrent engineering, model predictive control, and adaptive manufacturing.

Dynamic models of thermal management enable adjustments to external cooling or heating conditions. Simulations can help identify critical locations or cooling strategies for these auxiliary systems [88]. The control approach should match the manufacturing speed and production decision latency and process monitoring systems can be valuable. Simulations of temperature fields enable the prediction of energy consumption associated with cooling, heating, and temperature fields over different burial depths, enhancing strategy selection. The quantification of uncertainty of the temperature field gives information on the needs of distribution when it comes to sensors. Cryogenic-free deep UV lithography. A suitable cooling plan can reduce the energy usage and provide a temperature field meeting sealing needs.

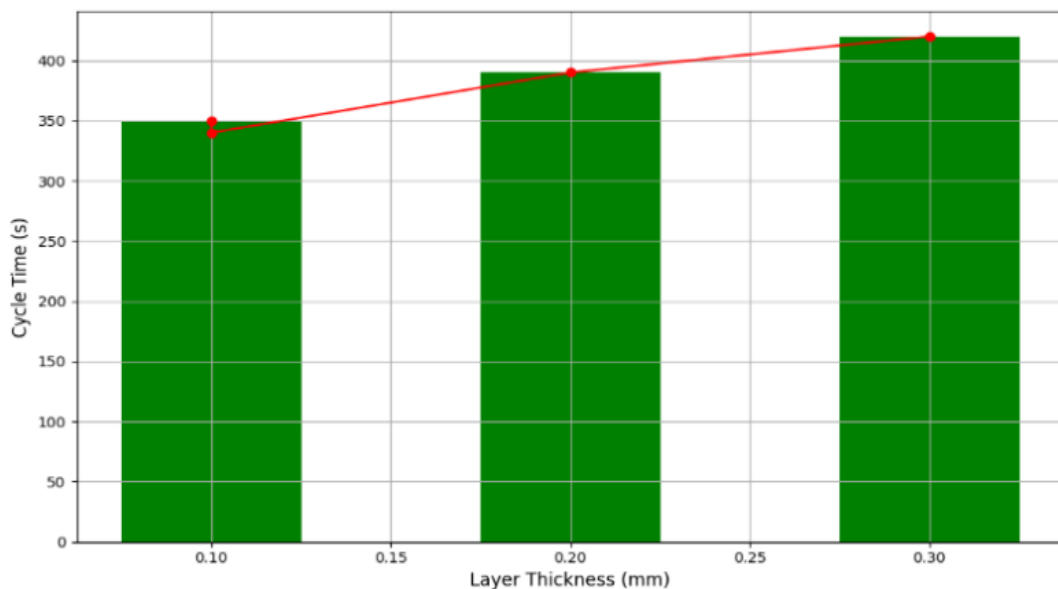
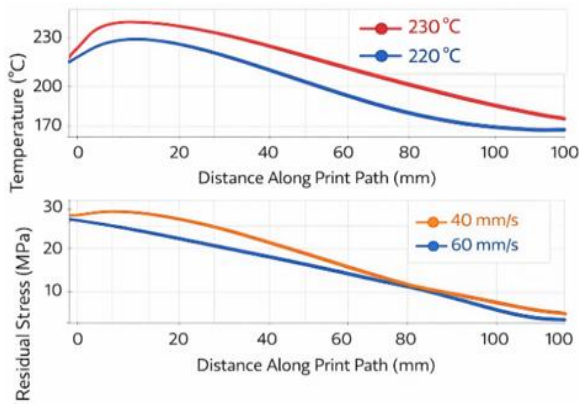
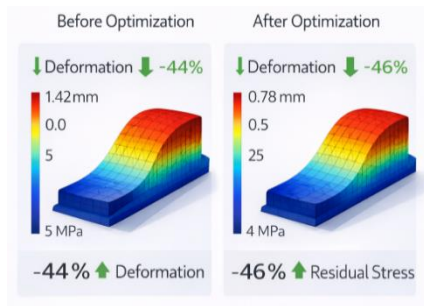


Figure 9. Influence of layer thickness on cycle time in 3D printing



**Figure 10.** Effect of extrusion temperature and print speed on temperature distribution and remaining stress along the print path



**Figure 11.** Before and after optimization of deformation and residual stress in 3D simulation

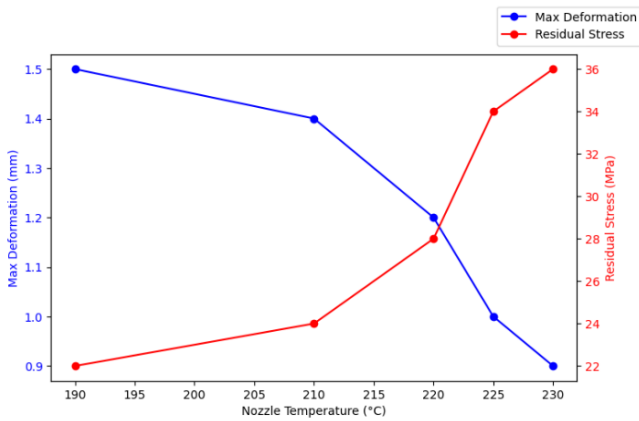


**Figure 12.** Effect of nozzle temperature on maximal deformation and residual stress in additive manufacturing processes

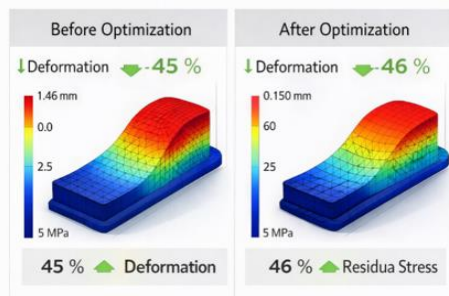


**Figure 13.** Thermal expansion analysis and multi-objective optimization in additive manufacturing processes: Deformation and energy consumption analysis

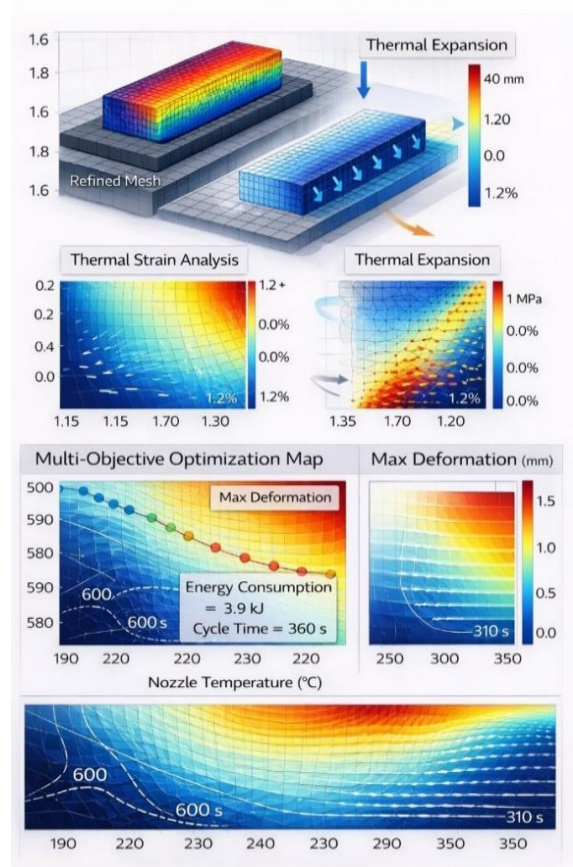


**Figure 14.** Comparison of deformation and residual stress before and after optimization in 3D simulation

**Table 12.** Optimization of 3D printing parameters before and after optimization

| Parameter       | Before Optimization | After Optimization | Change (%) |
|-----------------|---------------------|--------------------|------------|
| Nozzle Temp.    | 200 °C              | 215 °C             | 7.5%       |
| Printing Speed  | 40 mm/s             | 60 mm/s            | 50%        |
| Layer Thickness | 0.2 mm              | 0.25 mm            | 23%        |
| Cooling Time    | 6.0 s               | 3.5 s              | 42%        |

To evaluate the effectiveness of the optimization process, Table 12 presents a detailed comparison of key variables, such as nozzle temperature, printing speed, and layer thickness. As shown in the table, the strategic adjustments led to a notable decrease in cycle time from 480 s to 360 s, alongside improved cooling efficiency.

#### 4.7 Coatings and surface engineering

Molecular and colloidal chemical processes dictate the reliability and quality of thin functional surfaces and coatings. As shown in Table 10, adhesion strength, wear resistance, and protection against oxidation and corrosion depend on material selection and on suitability for the specific operating environment. Adequate simulation of functional film and coating formation requires, in essence, a coherent physical description of the relevant chemical and mass transport phenomena as well as the key physicochemical features of the environment. Thus, attention must often focus on chemical

kinetics and mass transport in films as well as in growth processes.

Published results suggest that, at least in thin films such as converters, fuel cells, and micro-electro-mechanical systems (MEMS) devices, mass transport frequently meets the required conditions for diffusion-limited kinetics. In such cases, chemical reactions proceed sufficiently fast to be governed either by diffusion-limited or kinetic-limited stages. Nevertheless, the integrated effect of reaction and mass transport appears insufficiently understood for many applications. For proustite coatings, reaction–diffusion problems contain considerable complexity, especially with regard to scratched parts' self-repairing capability and anticorrosion function in practical service [89]. As the environment heavily influences the kinetics and mass transport of reactions in every real process, it follows that the selected chemical description must take all relevant environmental parameters into account. So, the real field and service conditions must guide functional reproduction and quality prediction in practical application [90].

## 5. IMPLICATIONS FOR PRODUCTION EFFICIENCY AND SUSTAINABILITY

Evidence-based modeling and optimization of manufacturing processes directly enhance production efficiency by reducing economic expenditures in each machining component. Development effort concentrated on modelling surface integrity and quality loss for representative hard metal cutting, associating specific state parameters with the microstructural features and exploiting splat formation conditions for fast and wear-resistant thermal barrier coatings design [91]. Process parameters of high-rate laser cladding, influencing cooling rates and grain size, were identified using surrogate models for microstructure prediction trained on low-fidelity data. Temperature distributions in high-throughput reflow ovens were evaluated to propose cooling strategies balancing temperature uniformity and energy efficiency.

Well-targeted multiphysics simulations bring substantial improvements in production efficacy and process sustainability [92]. An objective function quantifying the machining energy consumption, acting as the primary input and a surrogate model for a preset criterion, enables real-time adaptation of production parameters in a rapidly changing environment with an unpredictable model state. Proper implementation of sensed data, minimization of decision latency, and suitable selection of a surrogate model ensemble guarantee consistent production efficiency across the considered application domain and establish a path towards autonomous predictive control.

## 6. CHALLENGES, LIMITATIONS, AND FUTURE DIRECTIONS

Designing and manufacturing goods with minimal negative environmental impact remains a major challenge. Limited resources dictate that unused time in factories worldwide must be minimized. A suggestion to conceive factories that reuse each other's wasted heat must be highlighted [93]. An experiment to demonstrate that the power used in data hosting alone surpasses the power per capita of countries is transformed into an enigma, requiring a shrinking of the data

used in hosting nowadays. The implications that surface treatment has on the thinning of natural resources and the negative impact that wear introduces on productivity, environment and resources are summarized.

Combined heat and mass transfers and chemical reactions have to be addressed through research and manufacturing. Surfaces should be coated in order to increase the life of tools and equipment; in each case, when an inorganic coating is used, the dangers attached must be compared to the advantages in terms of resources. Last but not least, brain(s) and speed might not be sufficient to spare other people suffering. The changes that this way of thinking dictates are presented as being on the agenda, which will allow an extended, further-reaching discussion.

## 7. CONCLUSIONS

Development of rigorous modeling and modeling applications in a wide variety of manufacturing settings drives multiphysics modeling, numerical modeling, validation and optimization approaches. Formalization of the simulation and optimization structures of the manufacturing process, and by applying multiphysics modeling strategically, one can increase the strength of the production processes, as well as enable control over the quality of the products with precision. The developed approaches, when applied, can result in quantifiable production efficiency improvement and surface integrity-related rework mitigation.

Production is entering a new era where cost and performance are not the only factors that should determine the design and manufacturing of products, but also the demands of the circular economy. The recent advancements in sensors, machine learning, and monitoring product quality have created new opportunities in real-time optimization of the manufacturing process, with the opening of the possibilities of reducing costs. Some of the aspects that may be correlated with the responsiveness of the process to current conditions include tool life, cooling, deposition rate and dimensional accuracy, just to mention a few. The incorporation of sensor information into sophisticated computational models can be used to make predictions of how a process will behave in various circumstances; this inevitably draws us to the idea of model predictive control.

From a manufacturing perspective, the thermo-mechanical optimization framework suggested here is an actual digital tool that can improve reliability, efficiency, and energy performance in the FDM processes. This study contributes to the industrialization of additive manufacturing technologies by actively promoting the use of data-driven process design and value addition by directly relating process parameters and performance indicators that are relevant to manufacturing.

## REFERENCES

- [1] Bellehumeur, C., Li, L., Sun, Q., Gu, P. (2004). Modeling of bond formation between polymer filaments in the fused deposition modeling process. *Journal of Manufacturing Processes*, 6(2): 170-178. [https://doi.org/10.1016/S1526-6125\(04\)70071-7](https://doi.org/10.1016/S1526-6125(04)70071-7)
- [2] Sun, Q., Rizvi, G.M., Bellehumeur, C.T., Gu, P. (2008). Effect of processing conditions on the bonding quality of FDM polymer filaments. *Rapid Prototyping Journal*,

- 14(2): 72-80. <https://doi.org/10.1108/13552540810862028>
- [3] Kousiatza, C., Karalekas, D. (2016). In-situ monitoring of strain and temperature distributions during fused deposition modeling process. *Materials & Design*, 97: 400-406. <https://doi.org/10.1016/j.matdes.2016.02.099>
- [4] Seppala, J.E., Migler, K.D. (2016). Infrared thermography of welding zones produced by polymer extrusion additive manufacturing. *Additive Manufacturing*, 12(Part A): 71-76. <https://doi.org/10.1016/j.addma.2016.06.007>
- [5] Coogan, T.J., Kazmer, D.O. (2017). Healing simulation for bond strength prediction of FDM. *Rapid Prototyping Journal*, 23(3): 551-561. <https://doi.org/10.1108/RPJ-03-2016-0051>
- [6] Garzon-Hernandez, S., Garcia-Gonzalez, D., Jérusalem, A., Arias, A. (2020). Design of FDM 3D printed polymers: An experimental-modelling methodology for the prediction of mechanical properties. *Materials & Design*, 188: 108414. <https://doi.org/10.1016/j.matdes.2019.108414>
- [7] Wang, J., Papadopoulos, P. (2021). Coupled thermomechanical analysis of fused deposition using the finite element method. *Finite Elements in Analysis and Design*, 197: 103607. <https://doi.org/10.1016/j.finel.2021.103607>
- [8] Samy, A.A., Golbang, A., Harkin-Jones, E., Archer, E., Tormey, D., McIlhagger, A. (2021). Finite element analysis of residual stress and warpage in a 3D printed semi-crystalline polymer: Effect of ambient temperature and nozzle speed. *Journal of Manufacturing Processes*, 70: 389-399. <https://doi.org/10.1016/j.jmapro.2021.08.054>
- [9] Samy, A.A., Golbang, A., Harkin-Jones, E., Archer, E., Tormey, D., McIlhagger, A. (2022). Influence of raster pattern on residual stress and part distortion in FDM of semi-crystalline polymers: A simulation study. *Polymers*, 14(13): 2746. <https://doi.org/10.3390/polym14132746>
- [10] Khanafer, K., Al-Masri, A., Deiab, I., Vafai, K. (2022). Thermal analysis of fused deposition modeling process based on finite element method: Simulation and parametric study. *Numerical Heat Transfer, Part A: Applications*, 81(3-6): 94-118. <https://doi.org/10.1080/10407782.2022.2038972>
- [11] Pedersen, D.B., Serdeczny, M.P. (2018). Thermo-mechanical implications of toolpath planning in fused filament fabrication. *Additive Manufacturing*, 22: 297-306. <https://doi.org/10.1016/j.addma.2018.05.012>
- [12] Gao, X., Qi, S., Kuang, X., Su, Y., Li, J., Wang, D. (2021). Fused filament fabrication of polymer materials: A review of interlayer bond. *Additive Manufacturing*, 37: 101658. <https://doi.org/10.1016/j.addma.2020.101658>
- [13] Vaes, D., Coppens, M., Goderis, B., Zoetelief, W., Van Puyvelde, P. (2021). The extent of interlayer bond strength during fused filament fabrication of nylon copolymers: An interplay between thermal history and crystalline morphology. *Polymers*, 13(16): 2677. <https://doi.org/10.3390/polym13162677>
- [14] Jiang, B., Chen, Y., Ye, L., Chang, L., Dong, H. (2023). Residual stress and warpage of additively manufactured SCF/PLA composite parts. *Advanced Manufacturing: Polymer & Composites Science*, 9(1): 2171940. <https://doi.org/10.1080/20550340.2023.2171940>
- [15] Lukhi, M., Mittermeier, C., Kiendl, J. (2025). Multi-physics simulation of a material extrusion-based additive manufacturing process: Towards understanding stress formation in the printed strand. *Progress in Additive Manufacturing*, 10(9): 6839-6853. <https://doi.org/10.1007/s40964-025-01012-9>
- [16] Mi, Y., Hashemi Sohi, S.H. (2025). Simulation analysis of temperature change in FDM process based on ANSYS APDL and birth-death element technology. *Micromachines*, 16(10): 1181. <https://doi.org/10.3390/mi16101181>
- [17] Farh, M.M., Gribniak, V. (2025). Thermo-mechanical approach to material extrusion process during fused filament fabrication of polymeric samples. *Materials*, 18(19): 4537. <https://doi.org/10.3390/ma18194537>
- [18] Conceição, M.N., Fonseca, H.M.D., Thiré, R.M.S.M. (2024). Temperature profile from parts produced by fused filament fabrication (FFF) measured by in situ infrared thermography. *Processes*, 13(1): 60. <https://doi.org/10.3390/pr13010060>
- [19] Meng, J., Liu, J., Xia, H., Ao, X., Zhang, W. (2025). A part-level simulation method considering thermal-mechanical contact between multiple filaments for material extrusion processes. *Virtual and Physical Prototyping*, 20(1): e2441944. <https://doi.org/10.1080/17452759.2024.2441944>
- [20] Oelsch, E., Landgraf, R., Ihlemann, J. (2021). A thermomechanical simulation method for fused filament fabrication with stepwise element activation. *Proceedings in Applied Mathematics and Mechanics*, 20(1): e202000206. <https://doi.org/10.1002/pamm.202000206>
- [21] Liao, Y., Jiang, Y. (2020). Multiphysics simulation and optimization of additive manufacturing processes. *Journal of Manufacturing Science and Engineering*, 142(10): 101011. <https://doi.org/10.1115/1.4047806>
- [22] Denlinger, E.R., Irwin, J., Michaleris, P. (2014). Thermomechanical modeling of additive manufacturing large parts. *Journal of Manufacturing Science and Engineering*, 136(6): 061007. <https://doi.org/10.1115/1.4028669>
- [23] Tapia, G., Elwany, A. (2014). A review on process monitoring and control in metal-based additive manufacturing. *Journal of Manufacturing Science and Engineering*, 136(6): 060801. <https://doi.org/10.1115/1.4028540>
- [24] Aggarangsi, P., Beuth, J.L. (2006). Localized preheating approaches for reducing residual stress in additive manufacturing. *Journal of Manufacturing Science and Engineering*, 128(4): 948-959. <https://doi.org/10.1115/1.2349691>
- [25] Parry, L., Ashcroft, I., Wildman, R. (2016). Understanding the effect of laser scan strategy on residual stress. *Additive Manufacturing*, 12: 1-15. <https://doi.org/10.1016/j.addma.2016.05.001>
- [26] Chiumenti, M., Neiva, E., Salsi, E., Cervera, M., Badia, S., Moya, J., Chen, Z. (2017). Numerical modelling and experimental validation of additive manufacturing by selective laser melting. *Additive Manufacturing*, 18: 171-185. <https://doi.org/10.1016/j.addma.2017.10.003>
- [27] Denlinger, E.R., Heigel, J.C., Michaleris, P., Palmer, T.A. (2015). Effect of inter-layer dwell time on distortion and residual stress in additive manufacturing of titanium

- and nickel alloys. *Journal of Materials Processing Technology*, 215: 123-131. <https://doi.org/10.1016/j.jmatprotec.2014.07.030>
- [28] Zander, N.E., Gillan, M., Lambeth, R.H. (2018). Recycled polyethylene terephthalate as a new FFF feedstock material. *Additive Manufacturing*, 21: 174-182. <https://doi.org/10.1016/j.addma.2018.03.007>
- [29] Ancellotti, S., Fontanari, V., Molinari, A., Iacob, E., et al. (2019). Numerical/experimental strategies to infer enhanced liquid thermal conductivity and roughness in laser powder-bed fusion processes. *Additive Manufacturing*, 27: 552-564. <https://doi.org/10.1016/j.addma.2019.04.007>
- [30] Gaikwad, A., Giera, B., Guss, G.M., Forien, J.B., Matthews, M.J., Rao, P. (2020). Heterogeneous sensing and scientific machine learning for quality assurance in laser powder bed fusion—A single-track study. *Additive Manufacturing*, 36: 101659. <https://doi.org/10.1016/j.addma.2020.101659>
- [31] Chen, Q., Zhao, Y., Strayer, S., Zhao, Y., et al. (2021). Elucidating the effect of preheating temperature on melt pool morphology variation in Inconel 718 laser powder bed fusion via simulation and experiment. *Additive Manufacturing*, 37: 101642. <https://doi.org/10.1016/j.addma.2020.101642>
- [32] Vijayavenkataraman, S., Kuan, L.Y., Lu, W.F. (2020). 3D-printed ceramic triply periodic minimal surface structures for design of functionally graded bone implants. *Materials & Design*, 191: 108602. <https://doi.org/10.1016/j.matdes.2020.108602>
- [33] Liu, J.H., Vanderesse, N., Stinville, J.C., Pollock, T.M., Bocher, P., Texier, D. (2019). In-plane and out-of-plane deformation at the sub-grain scale in polycrystalline materials assessed by confocal microscopy. *Acta Materialia*, 169: 260-274. <https://doi.org/10.1016/j.actamat.2019.03.001>
- [34] Cattenone, A., Morganti, S., Alaimo, G., Auricchio, F. (2019). Finite element analysis of additive manufacturing based on fused deposition modeling: Distortions prediction and comparison with experimental data. *Journal of Manufacturing Science and Engineering*, 141(1): 011010. <https://doi.org/10.1115/1.4041626>
- [35] Moradi, M., Hashemi, R., Kasaeian-Naeini, M. (2023). Experimental investigation of parameters in fused filament fabrication 3D printing process of ABS plus using response surface methodology. *The International Journal of Advanced Manufacturing Technology*, 126(5-6): 2595-2612. <https://doi.org/10.1007/s00170-023-11468-0>
- [36] Chen, G.G., Wang, D.S., Hua, W.J., Wu, W.B., Zhou, W.Y., Jin, Y.F., Zheng, W.X. (2023). Simulating and predicting the part warping in fused deposition modeling by thermal-structural coupling analysis. *3D Printing and Additive Manufacturing*, 10(1): 70-82. <https://doi.org/10.1089/3dp.2021.0119>
- [37] Khairallah, S.A., Anderson, A.T., Rubenchik, A., King, W.E. (2016). Laser powder-bed fusion additive manufacturing: Physics of complex melt flow and formation mechanisms of pores, spatter, and denudation zones. *Acta Materialia*, 108: 36-45. <https://doi.org/10.1016/j.actamat.2016.02.014>
- [38] Gusarov, A.V., Yadroitsev, I., Bertrand, P., Smurov, I. (2009). Heat transfer modelling and stability analysis of selective laser melting. *Applied Surface Science*, 254(4): 975-979. <https://doi.org/10.1016/j.apsusc.2007.08.101>
- [39] Herzog, D., Seyda, V., Wycisk, E., Emmelmann, C. (2016). Additive manufacturing of metals. *Acta Materialia*, 117: 371-392. <https://doi.org/10.1016/j.actamat.2016.07.019>
- [40] DebRoy, T., Wei, H.L., Zuback, J.S., Mukherjee, T., et al. (2018). Additive manufacturing of metallic components—Process, structure and properties. *Progress in Materials Science*, 92: 112-224. <https://doi.org/10.1016/j.pmatsci.2017.10.001>
- [41] Markl, M., Körner, C. (2016). Multiscale modeling of powder bed-based additive manufacturing. *Annual Review of Materials Research*, 46: 93-123. <https://doi.org/10.1146/annurev-matsci-070115-032158>
- [42] Marler, R.T., Arora, J.S. (2004). Survey of multi-objective optimization methods. *Structural and Multidisciplinary Optimization*, 26: 369-395. <https://doi.org/10.1007/s00158-003-0368-6>
- [43] Mansour, M.M., Erabee, I.K., Lafta, A.M. (2024). Comprehensive analysis of water based emulsion drilling fluids in GHARRAF oil field in southern Iraq: Properties, specifications, and practical applications. *International Journal of Computational Methods and Experimental Measurements*, 12(3): 297-307. <https://doi.org/10.18280/ijcmem.120310>
- [44] Mansour, M.M., Doos, Q.M. (2025). Developing expert system for defects diagnostic for specific oil refinery pipelines via using artificial neural network. *AIP Conference Proceedings*, 3303(1): 060010. <https://doi.org/10.1063/5.0261530>
- [45] Mansour, M. (2025). Assessing the role of circular economy principles in reducing waste by sustainable manufacturing practices: A review. *Sigma Journal of Engineering and Natural Sciences—Sigma Mühendislik Ve Fen Bilimleri Dergisi*, 43(5): 1886-1896. <https://doi.org/10.14744/sigma.2024.00155>
- [46] Lafta, A.M., Mansour, M.M. (2025). Employing artificial neural networks to forecast gas consumption by a power plant. *Academic Journal of Manufacturing Engineering*, 23(1): 72-86. <https://doi.org/10.5281/zenodo.15180611>
- [47] Ibrahim, Z.A., Mansour, M.M., Lafta, A.M., Uгла, A.A. (2024). Numerical investigation to evaluate the extrusion process of power cable designed by CFD software. *International Review of Mechanical Engineering*, 18(8): 384. <https://doi.org/10.15866/ireme.v18i8.24443>
- [48] Mansour, M.M. (2024). Using sustainable technique to recycle waste paper in academic institutions. *Al-Bahir*, 5(1): 5. <https://doi.org/10.55810/2313-0083.1069>
- [49] Mansour, M.M., Salman, A.M., Lafta, A.M. (2025). Innovative design and finite element analysis of wheel rims using boron epoxy composites: A cost-benefit and lifecycle assessment for industrial applicability. *Revue des Composites et des Matériaux Avancés—Journal of Composite and Advanced Materials*, 35(4): 709-723. <https://doi.org/10.18280/rcma.350413>
- [50] Mansour, M.M., Shkarah, A.J. (2025). Utilization of magnetic spheres in porous media for real-time control of heat dissipation. *International Communications in Heat and Mass Transfer*, 168: 109439. <https://doi.org/10.1016/j.icheatmasstransfer.2025.109439>
- [51] Erabee, I.K., Mansour, M.M., Lafta, A.M. (2025). Environmental impact of oil spills on water resources

- altering physical properties and treatment approaches. *Applied Chemical Engineering*, 8(3): 5692. <https://doi.org/10.59429/ace.v8i3.5692>
- [52] Shkarah, A.J., Noori, S.W., Lafta, D.A., Lafta, A.M., Mansour, M.M. (2025). Application of the homotopy perturbation method to the Jeffery-Hamel flow of nanofluids between two non-parallel planar walls. *Results in Engineering*, 28: 107805. <https://doi.org/10.1016/j.rineng.2025.107805>
- [53] Mansour, M.M., Uгла, A.A., Tahir, A.H., Lafta, A.M. (2025). Failure analysis for expansion joint in crude oil storage tank: Case study. *Sigma Journal of Engineering and Natural Sciences - Sigma Mühendislik ve Fen Bilimleri Dergisi*. <https://doi.org/10.14744/sigma.2025.1909>
- [54] Lafta, A.M., Mansour, M.M., Hamood, H.M. (2025). Numerical investigation of performance study of a solar stepped still using desalination system with cooling. *AIP Conference Proceedings*, 3303(1): 060011. <https://doi.org/10.1063/5.0263005>
- [55] Mansour, M.M. (2026). Recent advancements in refractory materials and digital innovations in precision manufacturing. *Sigma*, 44(2): 1509-1525. <https://doi.org/10.14744/sigma.2025.00096>
- [56] Salman, A.M., Mansour, M.M. (2025). Optimizing 3D printing processes by applying the Taguchi method for enhanced efficiency. *Academic Journal of Manufacturing Engineering*, 23(3): 136. <https://doi.org/10.5281/zenodo.17217531>
- [57] Lafta, D.A., Lafta, A.M., Noori, S.W., Mansour, M.M. (2026). Shadow assisted solar still: Surface cooling via sub-basin heat exchanger. *Results in Engineering*, 29: 108508. <https://doi.org/10.1016/j.rineng.2025.108508>
- [58] Abeykoon, C., Sri-Amphorn, P., Fernando, A. (2020). Optimization of fused deposition modeling parameters for improved PLA and ABS 3D printed structures. *International Journal of Lightweight Materials and Manufacture*, 3(3): 284-297. <https://doi.org/10.1016/j.ijlmm.2020.03.003>
- [59] Biswal, H.J., Metcalf, M., Stefanescu, C., Lucon, P. (2024). Development of a laser-assisted fused deposition modeling process for improvement in bond tensile strength of ABS. *Journal of Polymer Science*, 62(11): 2503-2514. <https://doi.org/10.1002/pol.20230926>
- [60] Buj-Corral, I., Domínguez-Fernández, A., Durán-Llucía, R. (2019). Influence of print orientation on surface roughness in fused deposition modeling (FDM) processes. *Materials*, 12(23): 3834. <https://doi.org/10.3390/ma12233834>
- [61] Mansour, M.M., Uгла, A.A. (2024). Employing genetic algorithm to optimize manufacturing cells design. *Academic Journal of Manufacturing Engineering*, 22(3): 53-61. [https://www.ajme.ro/PDF\\_AJME\\_2024\\_3/L7.pdf](https://www.ajme.ro/PDF_AJME_2024_3/L7.pdf)
- [62] Comminal, R., Serdeczny, M.P., Pedersen, D.B., Spangenberg, J. (2018). Numerical modeling of the strand deposition flow in fused filament fabrication. *Additive Manufacturing*, 20: 68-76. <https://doi.org/10.1016/j.addma.2017.12.013>
- [63] Costa, S.F., Duarte, F.M., Covas, J.A. (2015). Thermal conditions affecting heat transfer in FDM/FFE: A contribution towards the numerical modelling of the process. *Virtual and Physical Prototyping*, 10(1): 35-46. <https://doi.org/10.1080/17452759.2014.984042>
- [64] Costa, S.F., Duarte, F.M., Covas, J.A. (2017). Estimation of filament temperature and adhesion development in fused deposition techniques. *Journal of Materials Processing Technology*, 245: 167-179. <https://doi.org/10.1016/j.jmatprotec.2017.02.026>
- [65] Costanzo, A., Arznumudian, M., Downing, J.M., Smith, P. (2020). Residual alignment and its effect on weld strength in material-extrusion 3D-printing of polylactic acid. *Additive Manufacturing*, 36: 101503. <https://doi.org/10.1016/j.addma.2020.101503>
- [66] Enriconi, L., Bonaiti, L., Ghidini, T. (2025). Numerical simulation and optimization trends in fused filament fabrication: Thermal-mechanical viewpoints. *Applied Sciences*, 15(12): 6696. <https://doi.org/10.3390/app15126696>
- [67] Greeff, G.P., Schilling, N. (2018). Single print optimisation of fused filament fabrication parameters. *The International Journal of Advanced Manufacturing Technology*, 99: 845-856. <https://doi.org/10.1007/s00170-018-2518-4>
- [68] Gosset, A., Barreiro-Villaverde, D., Becerra Permy, J.C., Lema, M., Ares-Pernas, A., Abad López, M.J. (2020). Experimental and numerical investigation of the extrusion and deposition process of a poly (lactic acid) strand with fused deposition modeling. *Polymers*, 12(12): 2885. <https://doi.org/10.3390/polym12122885>
- [69] Han, P., Zhang, Y., Liu, H., Wang, X. (2023). In-process orbiting laser-assisted technique for surface finish in material extrusion-based 3D printing. *Polymers*, 15(9): 2221. <https://doi.org/10.3390/polym15092221>
- [70] Jeon, S., Park, S.J., Moon, S.K., Yang, D. (2025). Enhanced mechanical properties and reduced anisotropy of material extrusion-manufactured short carbon fibre-reinforced plastic via cold isostatic pressing. *Virtual and Physical Prototyping*, 20(1): e2499934. <https://doi.org/10.1080/17452759.2025.2499934>
- [71] Koker, B., Ruckdashel, R., Abajorga, H., Curcuru, N., et al. (2022). Enhanced interlayer strength and thermal stability via dual material filament for material extrusion additive manufacturing. *Additive Manufacturing*, 55: 102807. <https://doi.org/10.1016/j.addma.2022.102208>
- [72] Kumar, M.S., Farooq, M.U., Ross, N.S., Yang, C.H., Kavimani, V., Adedirán, A.A. (2023). Achieving effective interlayer bonding of PLA parts during the material extrusion process with enhanced mechanical properties. *Scientific Reports*, 13: 6800. <https://doi.org/10.1038/s41598-023-33510-7>
- [73] Lou, X., Tang, X. A., Dong, L., Zhao, T., Wang, F., Zhao, L., Zhang, T. (2025). Influence of layer thickness and extrusion ratio on strand morphology, porosity, surface roughness, and anisotropic mechanical properties in FDM. *Scientific Reports*, 15(1): 42351. <https://doi.org/10.1038/s41598-025-26253-0>
- [74] Jerez-Mesa, R., Travieso-Rodríguez, J., Corbella, X., Busqué, R., Gomez-Gras, G. (2016). Finite element analysis of the thermal behavior of a RepRap 3D printer liquefier. *Mechatronics*, 36: 119-126. <https://doi.org/10.1016/j.mechatronics.2016.04.007>
- [75] Mohamed, O.A., Masood, S.H., Bhowmik, J.L. (2015). Optimization of fused deposition modeling process parameters: A review of current research and future prospects. *Advances in Manufacturing*, 3: 42-53. <https://doi.org/10.1007/s40436-014-0097-7>
- [76] Morvayová, A., Contuzzi, N., Casalino, G. (2023).

- Defects and residual stresses finite element prediction of FDM 3D printed wood/PLA biocomposite. *The International Journal of Advanced Manufacturing Technology*, 129(5): 2281-2293. <https://doi.org/10.1007/s00170-023-12410-0>
- [77] Ramos, N., Mittermeier, C., Kiendl, J. (2023). Efficient simulation of the heat transfer in fused filament fabrication. *Journal of Manufacturing Processes*, 94: 550-563. <https://doi.org/10.1016/j.jmapro.2023.03.030>
- [78] Omer, M.A., Shaban, I.A., Mourad, A.H., Hegab, H. (2025). Advances in interlayer bonding in fused deposition modelling: A comprehensive review. *Virtual and Physical Prototyping*, 20(1): e2522951. <https://doi.org/10.1080/17452759.2025.2522951>
- [79] Oskolkov, N., Smirnov, A., Kuznetsov, D. (2023). Thermal and mechanical behavior of material-extrusion printed polymers: A process-property perspective. *Polymers*, 15(23): 4518. <https://doi.org/10.3390/polym15234518>
- [80] Parandoush, P., Lin, D. (2017). A review on additive manufacturing of polymer-fiber composites. *Composite Structures*, 182: 36-53. <https://doi.org/10.1016/j.compstruct.2017.08.088>
- [81] Peterson, A.M., Kazmer, D.O. (2022). Effective interlayer diffusion and weld formation mechanisms in material extrusion. *Scientific Reports*, 12: 19053. <https://doi.org/10.1038/s41598-022-19053-3>
- [82] Ravi, A.K., Deshpande, A., Hsu, K. (2016). In-process laser localized pre-deposition heating: Interlayer bond strengthening in extrusion-based polymer additive manufacturing. *Journal of Manufacturing Processes*, 24: 179-185. <https://doi.org/10.1016/j.jmapro.2016.08.007>
- [83] Pollard, D., Jolly, M., Cleary, P. (2017). Simulation of polymer deposition for fused filament fabrication. *Procedia Manufacturing*, 11: 1426-1434. <https://doi.org/10.1016/j.promfg.2017.07.147>
- [84] Aadithyan, A., Shnain, A.H., Sharma, V., Lafta, A.M., Mudhafar, M., Ghobash, A., Jawad, A.Q. (2024). The technical ethics used in bad and SD methods: A deep review. In *2024 4th International Conference on Advance Computing and Innovative Technologies in Engineering (ICACITE)*, Greater Noida, India, pp. 1226-1230. <https://doi.org/10.1109/ICACITE60783.2024.10616634>
- [85] Santos, A., Ribeiro, P., Duarte, F. (2023). Insights into temperature simulation and validation of fused deposition modeling processes. *Journal of Manufacturing and Materials Processing*, 7(6): 189. <https://doi.org/10.3390/jmmp7060189>
- [86] Seppala, J.E., Migler, K.D. (2017). Infrared thermography of polymer cooling in material extrusion additive manufacturing. *Soft Matter*, 13(39): 6761-6768. <https://doi.org/10.1039/C7SM00950J>
- [87] Serdeczny, M.P., Comminal, R., Pedersen, D.B., Spangenberg, J. (2018). Experimental validation of deposition mechanics and bead geometry in fused filament fabrication. *Additive Manufacturing*, 24: 428-438. <https://doi.org/10.1016/j.addma.2018.10.005>
- [88] Shanmugam, V., Babu, K., Kannan, G., Mensah, R.A., Samantaray, S.K., Das, O. (2024). The thermal properties of FDM printed polymeric materials: A review. *Polymer Degradation and Stability*, 228: 110902. <https://doi.org/10.1016/j.polymdegradstab.2024.110902>
- [89] Syrlybayev, D., Zharylkassyn, B., Seisekulova, A., Perveen, A., Talamona, D. (2021). Optimization of the warpage of fused deposition modeling parts using finite element method. *Polymers*, 13(21): 3849. <https://doi.org/10.3390/polym13213849>
- [90] Tymrak, B.M., Kreiger, M., Pearce, J.M. (2014). Mechanical properties of components fabricated with open-source 3-D printers under realistic environmental conditions. *Materials & Design*, 58: 242-246. <https://doi.org/10.1016/j.matdes.2014.02.038>
- [91] Wickramasinghe, S., Do, T., Tran, P. (2020). FDM-based 3D printing of polymer and associated composite: A review on mechanical properties, defects and treatments. *Polymers*, 12(7): 1529. <https://doi.org/10.3390/polym12071529>
- [92] Yin, J., Lu, C., Fu, J., Huang, Y., Zheng, J. (2018). Interfacial bonding during fused filament fabrication: Effects of thermal history and process parameters. *Materials & Design*, 155: 324-333. <https://doi.org/10.1016/j.matdes.2018.04.029>
- [93] El Moumen, M., Tarfaoui, M., Lafdi, K. (2019). Modelling of the temperature and residual stress fields during 3D printing of polymer composites. *The International Journal of Advanced Manufacturing Technology*, 104: 1661-1674. <https://doi.org/10.1007/s00170-019-03965-y-102>